Materials for Renewable and Sustainable Energy (2019) 8:17
https://doi.org/10.1007/s40243-019-0155-y

ORIGINAL PAPER

Active Pt/CeO_2 catalysts prepared by an alcohol-reduction process for low-temperature CO-PROX reaction

Carla Moreira Santos Queiroz[1] · Arthur Pignataro Machado[1] · Ana Rita Noborikawa Paiva[1] · Rodolfo Molina Antoniassi[1,2] · Jorge Moreira Vaz[1] · Estevam Vitorio Spinacé[1]

Received: 20 May 2019 / Accepted: 20 August 2019 / Published online: 29 August 2019

Abstract

Pt/CeO_2 catalysts were prepared with 0.5 and 1 wt% of Pt loadings by an alcohol-reduction process using a solution of ethylene glycol and water as a reducing agent and solvent. The obtained catalysts were characterized by energy-dispersive X-ray spectroscopy, X-ray diffraction, and transmission electron microscopy. Transmission electron micrographs showed Pt nanoparticles with average sizes of 2.2 and 2.4 nm for Pt content of 0.5 and 1 wt%, respectively. The preferential oxidation of carbon monoxide in hydrogen-rich stream (CO-PROX reaction) was studied in the temperature range of 25–150 °C. Pt/CeO_2 catalysts showed maximum CO conversions in the range of 80–98% and CO_2 selectivity in the range of 50–70% at 50 °C.

Keywords Pt/CeO_2 catalysts · Alcohol-reduction process · Hydrogen · Carbon monoxide · CO-PROX reaction

Introduction

Nowadays, the hydrogen production worldwide is mainly employed in the ammonia synthesis reaction and there is an increasing interest as a clean combustible option for fuel cell technology [1]. Steam reforming of natural gas or the light oil fraction coupled with water gas shift reaction is the most widely used process to produce a H_2-rich gas mixture known as a reformate gas, which contains 15–20 vol% CO_2, 10 vol% H_2O, and ~ 1 vol% (10,000 ppm) of carbon monoxide (CO) [1, 2]. However, the catalysts used in the ammonia production and low-temperature fuel cell devices are very sensitive to CO. Therefore, H_2 must be high purity for both applications and the CO concentration must be decreased to less than 10 ppm [3–5]; although in some situations, CO levels between 50 and 100 ppm could be tolerated for use in proton exchange membrane (PEM) fuel cells. [1, 6].

Some processes have been used to remove CO from H_2-rich mixtures like pressure swing adsorption (PSA) that requires large capital investments and employ physic-sorbents to produce a very pure H_2 stream but with H_2 recovery values between 75 and 85% [1, 4, 5]. Another process is the methanation of CO (CO-MET), which operates at 300–400 °C, but causes significant loss of the produced hydrogen (10–15%) because of the unselective methanation of CO_2 present in the reformate gas [1]. In face of this, more efficient processes such as selective methanation of CO (CO-SMET) and the preferential CO oxidation reaction (CO-PROX) have been developed for producing high-purity hydrogen. The CO-SMET process is able to reduce the CO concentration at low levels using the H_2 itself present in the stream producing methane at temperatures ≥ 200 °C. The CO-SMET process tends to be more easily controllable, when compared to CO-PROX, since the CO and CO_2 methanation reactions are less exothermic than H_2 and CO oxidations; however, the H_2 consumption could be higher by about two times compared to the H_2 consumed for H_2O formation during CO-PROX processing [4–7]. Extensive research has been dedicated to the development of high selective catalysts to reduce the H_2 consume in the unselective CO_2 methanation [6, 7]. The CO-PROX process could avoid the hydrogen and energy loss, oxidizing CO at lower

✉ Jorge Moreira Vaz
jmvaz@ipen.br

✉ Estevam Vitorio Spinacé
espinace@ipen.br

1 Instituto de Pesquisas Energéticas e Nucleares, IPEN-CNEN/SP, Av. Prof. Lineu Prestes, 2242, Cidade Universitária, São Paulo, SP 05508-900, Brazil

2 Instituto de Química, Universidade de São Paulo, Av. Prof. Lineu Prestes, 748, Cidade Universitária, São Paulo, SP 05508-000, Brazil

temperatures (in the range of 20–200 °C) with O_2 as oxidant; however, the catalysts for CO-PROX process need to exhibit high CO conversion and CO_2 selectivity, avoiding the oxidation of H_2 to H_2O. Thus, the development of more active and selective catalysts for CO-PROX process continues to be a challenge [1, 2].

Platinum nanoparticles supported on ceria (Pt/CeO_2) catalysts are one of the most active catalysts for CO-PROX reaction, leading to the maximum CO conversions and good CO_2 selectivity in the temperature range between 60 and 150 °C. For these catalysts, the temperatures at which maximum CO conversion occurs, as well as the best CO_2 selectivity values, were strongly dependent on the catalyst preparation method [8–21].

In this work, Pt/CeO_2 catalysts were prepared by an alcohol-reduction process [22], resulting in a very small and highly dispersed Pt nanoparticles on CeO_2 support, showing good CO conversions and CO_2 selectivity at 50 °C.

Experimental

Catalyst preparation

Pt/CeO_2 catalysts were prepared by an alcohol-reduction process [22] with Pt contents of 0.5 and 1 wt%, named, respectively, as $Pt0.5/CeO_2$ and $Pt1/CeO_2$. In this process, CeO_2 support (nanopowder with particle size ≤ 25 nm from Sigma-Aldrich) was dispersed in a solution of ethylene glycol/water (3/1, vol/vol) followed by the addition of the Pt precursor (H_2PtCl_6 $6H_2O$—Sigma-Aldrich). The resulting mixture was placed in an ultrasonic bath for 5 min, and then, it was immersed in an oil bath and refluxed at about 150 °C under magnetic stirring. After 2 h under stirring at 150 °C, the mixture was cooled to room temperature and the solid was separated by centrifugation and washed with distilled water six times to remove chloride ions and reaction by-products. The obtained catalysts were dried overnight at 85 °C in an oven.

Characterization

The semi-quantitative chemical analysis of Pt/CeO_2 catalysts were performed by the energy-dispersive X-ray spectroscopy (EDX) using a Philips scanning microscope (model Jeol with electron beam of 20 keV) equipped with EDAX microanalyzer (model DX-4). The solid samples were deposited on the grids and the results refer to an average of four random points collected from each sample. For the study of morphological and structural properties, X-ray diffraction (XRD) and transmission electron microscopy (TEM) techniques were used. The crystalline structure of the catalysts was obtained in a Rigaku diffractometer model Miniflex II from $2\theta = 20$ to 90° with 0.05 step and 2 s count using Cu Kα radiation source ($\lambda = 1.54$ Å). The micrographs analysis was performed on transmission electron microscope model JEM-2100 (200 kV). For this, an aliquot of a suspension of the catalyst in 2-propanol was deposited on a copper grid (0.3 cm in diameter) with a carbon film. Eight micrographs were taken, allowing counting of about 200 Pt nanoparticles for each sample, to measure the sizes and particle-size distributions.

The temperature-programmed reduction (TPR) with H_2 measurements was performed on ChemBET Pulsar TPR/TPD chemisorption analyzer with a thermal conductivity detector (TCD). The catalysts (50 mg) in a U-shaped quartz cell were treated in a flow of N_2 (50 mL min^{-1}) at 200 °C for 1 h. After cooling to room temperature, the catalysts were exposed to 10% vol H_2/N_2 gas flow (30 mL min^{-1}) and heated to 900 °C with a heating rate of 10 °C min^{-1}.

Catalytic tests

CO-PROX reaction measurements were performed in gas phase, using a fixed bed reactor, containing 100 mg of catalyst. No catalyst activation treatment was performed prior to the catalytic experiments. The catalytic testing was conducted at atmospheric pressure and in two runs (cycles), each run in the temperature range from 20 to 150 °C. The experiments were performed with a gas stream consisting of 1 v% CO, 0.5–1 v% O_2, and 98–98.5 v% H_2, and flow rates of 25 mL min^{-1} (O_2/CO ratio of 1, space velocity of 15,000 mL g_{cat}^{-1} h^{-1}) and 50 mL min^{-1} (O_2/CO ratio of 0.5, space velocity of 30,000 mL g_{cat}^{-1} h^{-1}.) The reaction products and unconverted reagents were quantified by gas chromatography with TCD and FID (methanation of CO and CO_2) detectors. The CO and O_2 conversions and CO_2 selectivity were calculated according to the following equations:

$$\text{CO conversion} = 100 \times \left([\text{CO}]_{\text{in}} - [\text{CO}]_{\text{out}}\right) / [\text{CO}]_{\text{in}}, \tag{1}$$

$$\text{O}_2\ \text{Conversion} = 100 \times \left(\left[\text{O}_{2\text{in}}\right] - \left[\text{O}_{2\text{out}}\right] / \left[\text{O}_{2\text{in}}\right]\right), \tag{2}$$

$$\text{CO}_2\ \text{selectivity} = 100 \times \left(0.5 * \left[\text{CO}_2\right]_{\text{out}}\right) / \left(\left[\text{O}_2\right]_{\text{in}} - \left[\text{O}_2\right]_{\text{out}}\right), \tag{3}$$

for CO_2 selectivity, the number 0.5 refers to stoichiometric coefficient, where 1 mol of CO reacts with 0.5 mol of O_2 to produce 1 mol of CO_2.

Results and discussion

The EDX analysis of the Pt/CeO_2 catalysts (Table 1) showed that the obtained Pt values (wt%) were similar to the nominal values, suggesting that all Pt(IV) ions were reduced and deposited on the CeO_2 support.

Table 1 Chemical composition of Pt/CeO_2 catalysts

Catalysts	EDX analysis	
	Pt (wt%)	CeO_2 (wt%)
Pt0.5/CeO_2	0.6	99.4
Pt1/CeO_2	1.1	98.9

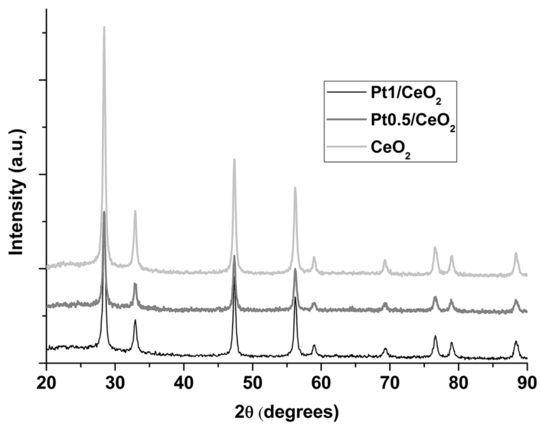

Fig. 1 X-ray diffractograms of CeO_2 support and Pt/CeO_2 catalysts

The X-ray diffractograms of Pt/CeO_2 catalysts are shown in Fig. 1. In these diffractograms, it was observed diffraction peaks at $2\theta = 28.3°$, 32.9°, 47.3°, 56.2°, 58.9°, 69.2°, 76.5°, 78.9°, and 88.3°, referring to the diffraction pattern of the ceria cubic crystalline phase (ICSD # 72155). On the other hand, no peaks relative to face-centered cubic (fcc) phase of Pt nanoparticles at $2\theta = 40°$, 47°, 67°, 82°, and 87° were observed [22]. Since the EDX analyses showed the presence of Pt in these catalysts, the absence of the Pt (fcc) peaks could be associated with a very small size of the nanoparticles. Thus, the small size and low contents (wt%) of Pt result in broad and low-intensity peaks that were too small to be clearly detected by XRD [9, 16].

The transmission electron micrographs and the histograms of Pt/CeO_2 catalysts are shown in Fig. 2. The TEM micrographs of Pt0.5/CeO_2 and Pt1/CeO_2 catalysts, Fig. 2a, b, respectively, showed spherical Pt nanoparticles highly dispersed on CeO_2 support with average sizes of 2.2 and 2.4 nm, respectively. This shows that this methodology is adequate to produce very small Pt nanoparticles highly dispersed on CeO_2 support as already observed in the preparation of Pt/C catalysts (20 wt% of Pt) for low-temperature fuel cells [22].

The H_2-TPR profiles of CeO_2 support and Pt/CeO_2 catalysts are shown in Fig. 3. As described in the literature [21,

Fig. 2 Transmission electron micrographs and histograms of (**a**) Pt0.5/CeO_2 and (**b**) Pt1/CeO_2

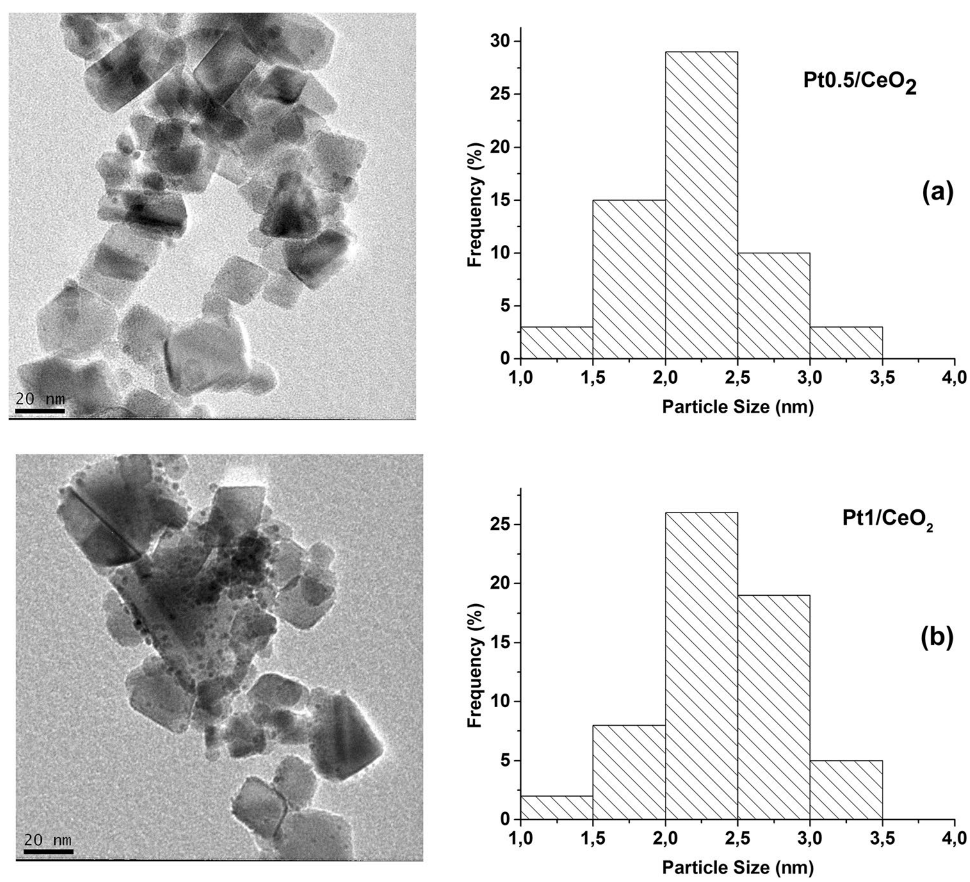

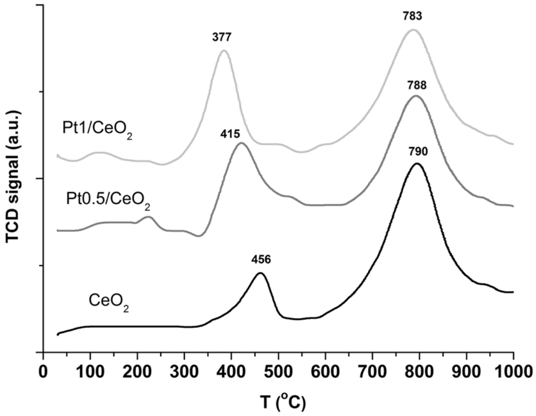

Fig. 3 H_2-TPR profiles of CeO_2 support and Pt/CeO_2 catalysts

23, 24], H_2-TPR profiles of Pt/CeO_2 catalysts showed three regions: the first one, in the range of 100–300 °C due to the reduction of PtO_x species to Pt(0) and/or to CeO_x species directly bonded to Pt reducing at lower temperatures; the second in the range of 300–600 °C assigned to the reduction of superficial CeO_x species; and the third in the region above 600 °C due to the bulk reduction of CeO_2. The H_2-TPR profile of CeO_2 support showed two reduction peaks: one at 456 °C assigned to the reduction of CeO_2 species on the surface and one at 790 °C within the bulk. Comparing H_2-TPR profiles of Pt/CeO_2 catalysts with the CeO_2 support, it can be seen the peak observed at 456 °C for CeO_2 support was shifted to 415 °C and 377 °C for Pt0.5/CeO_2 and Pt1/CeO_2 catalysts, respectively. This shift to lower temperatures indicated the existence of metal-support interactions, increasing the mobility of oxygen inside CeO_2 crystal lattice and improving the redox properties of the catalysts [21]. On the other hand, the peak at 790 °C observed for the CeO_2 support was practically in the same position for Pt/CeO_2 catalysts, which indicated that Pt did not influence the reduction of oxygen species within bulk of CeO_2 [23]. In addition, the H_2-TPR profiles of Pt/CeO_2 catalysts showed two small peaks in the range of 100–250 °C. Under the synthesis conditions of Pt/CeO_2 catalysts prepared by an alcohol-reduction process, the Pt(IV) ions are reduced to Pt(0), leading to the Pt nanoparticle formation [22], which suggest that these peaks could be attributed principally to CeO_x species directly bonded to Pt reducing at lower temperatures [21]. Thus, these results indicate that for Pt0.5/CeO_2 and Pt1/CeO_2 catalysts a strong metal-support interaction occurs preferentially on the surface of the CeO_2 than in the bulk.

The catalytic performances of Pt/CeO_2 are shown in Fig. 4a–c. No previous treatments were done in these samples and the results shown correspond to the second cycle of the catalytic reactions. In a general manner, for all catalysts, it was observed after the first cycle (from 25 to 150 °C) an increase of the performance of the catalysts principally at

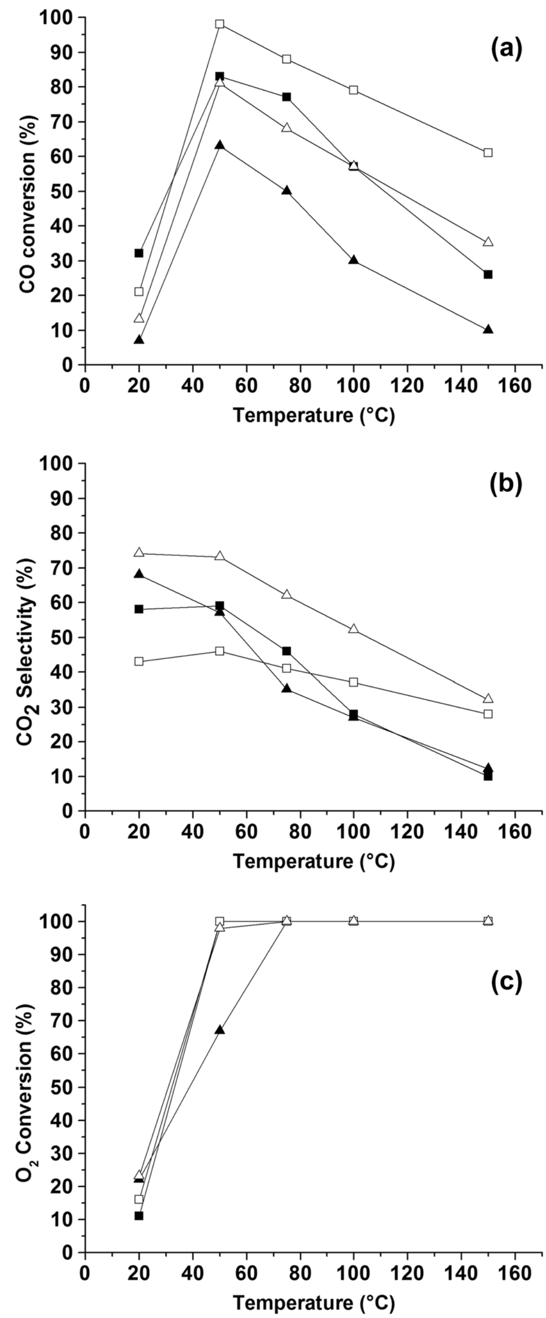

Fig. 4 Catalytic performance of Pt/CeO_2 catalysts: (**a**) CO conversion, (**b**) CO_2 selectivity, and (**c**) O_2 conversion (filled square Pt1/CeO_2 1% O_2, filled triangle Pt1/CeO_2 0.5% O_2, empty square Pt0.5/CeO_2 1% O_2, and empty triangle Pt0.5/CeO_2 0.5% O_2)

low temperatures (below 75 °C). Probably, this increase of performance at low temperature in the second cycle could be due to a decrease of Pt cationic species and/or to a surface cleaning of the catalysts which lead to a better accessibility of the Pt surface under reaction conditions. Above 75 °C, the values of CO and O_2 conversion and CO_2 selectivity practically did not change from the first to the second cycle.

Initially, the catalysts Pt0.5/CeO_2 and Pt1/CeO_2 were tested using a volumetric O_2/CO ratio of 1 ($\lambda = 2$ – excess of O_2). For both catalysts, the CO and O_2 conversions were very low (around 25%) at 25 °C. When the temperature was raised to 50 °C both the CO conversion and the O_2 consumed increased to 98% for Pt0.5/CeO_2 catalyst while for Pt1/CeO_2 catalyst, a CO conversion increased to 83% and 65% of the O_2 was consumed. For both catalysts, the CO_2 selectivity values were in the range of 45–55%. Above 75 °C, the O_2 was totally consumed for both catalysts; however, the CO conversion and CO_2 selectivity values begin to decrease continuously up to 150 °C due to the undesirable water formation. According to the literature [9], at low temperature, there is a complete coverage of the Pt surface by CO, which is oxidized to a greater extent as the O_2 content increases in the gas stream. When the temperature increases, desorption of CO from Pt surface becomes important and it is partially replaced by H_2, favoring its oxidation and consequently decreasing CO_2 selectivity.

Pt0.5/CeO_2 and Pt1/CeO_2 were also tested using a volumetric O_2/CO ratio of 0.5 ($\lambda = 1$). When tested under stoichiometric conditions, the maximum CO conversion continues to occur at 50 °C for both catalysts; however, an increase of CO_2 selectivity values was observed for Pt0.5/CeO_2 catalyst. Although CO conversion at 50 °C decreased from 98 to 81% when the O_2/CO ratio decreased from 1 to 0.5, the CO_2 selectivity increased from 46 to 73%. Wootsch et al. [8] using Pt/CeO_2 prepared by impregnation and O_2/CO ratios of 0.5 and 1 observed similar values of maximum CO conversion and CO_2 selectivity; nevertheless, these values were obtained at 100 °C, while for our catalysts, it occurred at 50 °C.

To evaluate the stability of the catalysts after the second cycle, long-term experiments were performed at 50 °C (Fig. 5a–c). In all cases, the CO conversion, O_2 conversion, and CO_2 selectivity values were very similar to the ones observed in the second cycle at 50 °C, and these values remained stable throughout the period evaluated.

Comparing our results with those reported in the literature (Table 2), it could be seen that most of Pt/CeO_2 catalysts showed maximum CO conversions at temperatures ≥ 80 °C. Only a few results [14, 16] described the maximum CO conversion at 60 °C but with CO_2 selectivity values ≤ 40%. Kugai et al. [14] prepared Pt/CeO_2 catalyst (2.2 wt% of Pt) by radiolytic process and obtained a maximum CO conversion of 100% at 60 °C using a high O_2/CO ratio of 2 ($\lambda = 4$), however, with a low CO_2 selectivity of 25%. Gao et al. [16] prepared Pt/CeO_2 catalysts with different Pt loadings and different morphologies of CeO_2 support by incipient wetness impregnation. The material prepared with 0.5 wt% of Pt and supported on rods CeO_2 showed a maximum CO conversion of 85% at 60 °C and CO_2 selectivity of 40% using an O_2/CO ratio of 1 ($\lambda = 2$).

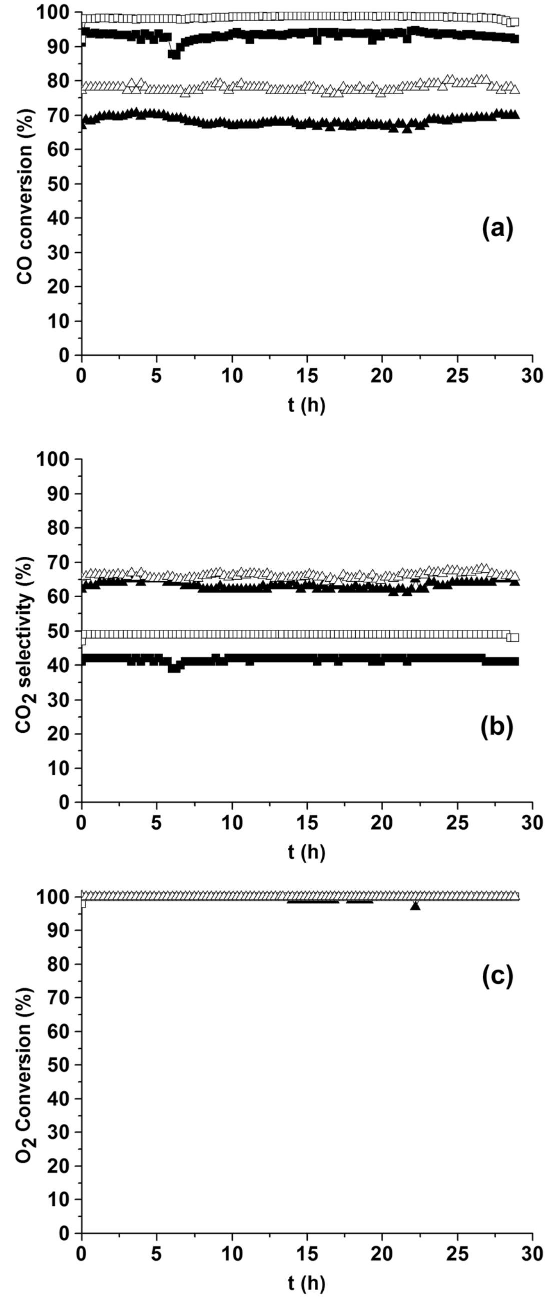

Fig. 5 Long-term tests of Pt/CeO_2 catalysts at 50 °C: (**a**) CO conversion, (**b**) CO_2 selectivity, and (**c**) O_2 conversion (filled square Pt1/CeO_2 1% O_2, filled triangle Pt1/CeO_2 0.5% O_2, empty square Pt0.5/CeO_2 1% O_2, and empty triangle Pt0.5/CeO_2 0.5% O_2)

The good performance of our Pt/CeO_2 catalysts (Pt nanoparticles supported on nanosized CeO_2) for CO-PROX reaction at 50 °C, perhaps, could be explained by the following factors: the small sizes of Pt nanoparticles and the strong metal-support interactions. Gatla et al. [25] described that nanosized CeO_2 has an important role as a catalyst support due to the great amount of surface oxygen defects and in particular oxygen ion vacancies that

Table 2 Comparison of the catalytic performance over Pt/CeO_2 catalysts for CO-PROX reaction reported in the literature

Method	Catalyst treatment process before reaction	Pt metal loading (wt%)/CeO2 support	Pt particle size (nm)/dispersion	Feed composition (vol%)	Space velocity or GHSV	O_2/CO feed ratio	λ	T (°C)[a]	CO conversion (%)	CO_2 selectivity (%)	References
Wet impregnation Pt(NH)3(OH)2	Calcined 450 °C in air reduced 400 °C in H_2	1 wt%, Rhodia catalysts and electronics	$D=53\%$	70% H_2, 5%CO, 2–5%O_2, He as balance	60,000 mL g^{-1} h^{-1}	0.5 1	1 2	100 100	78 95	80 48	[8]
Wet impregnation Pt(NH3)4(NO3)2	Calcined 400 °C in air reduced 300 °C in H_2	0, 54 wt%, Rhodia	$D=71.5\%$ 1.3 nm	1% CO, 60% H_2, 0–1.5% O_2 and He to balance	GHSV = 12,000 h^{-1}	0.5 1	1 2	90 80	55 94	55 47	[9]
Wet impregnation Pt(NH)3(OH)2	Calcined 500 °C in air reduced 400 °C in H_2	1 wt%, Rhodia, 96 m^2 g^{-1}	$D=62\%$	1% CO, 0.4–1% O_2, H_2 balance	73,170 mL g^{-1} h^{-1}	0.5 1	1 2	110 110	65 83	66 42	[10]
Wet impregnation Pt(NH)3(OH)2	Calcined 500 °C in air reduced 400 °C in H_2	1 wt% Rhodia, 96 m^2 g^{-1}	$D=62\%$	1% CO, 1% O_2, H_2 balance	GHSV = 16,000 h^{-1}	1	2	75	95	50	[11, 12]
Reduction–deposition (formaldehyde)	–	0.43 wt% CeO2 supports prepared by the urea gelation technique, BET area 16 m^2 g^{-1}	$D=61\%$	50% H_2, 1% CO, 0.5% O_2, balance He	60,000 mL g^{-1} h^{-1}	0.5	1	100	25	50	[13]
Radiolytic process	–	2.2 wt% CeO2 14 nm of average particle size, NanoTek, C. I. Kasei Co	3–4 nm	1% CO, 0.5–2% O2, 60–67.2% H_2, N_2 balance	30,000 mL g^{-1} h^{-1}	0.5 2	1 4	80 60	65 100	65 25	[14]
PVA/borohydride reduction	Calcined 400 °C in air Reduced 400 °C in H_2	1 wt%, Three-dimensionally ordered macro- and meso-porous CeO_2	5 nm	1.0% CO, 1.0%O_2, 50% H_2 (He balanced)	30,000 mL g^{-1} h^{-1}	1	2	70	85	85	[15]
Incipient wetness impregnation	Reduced 200 °C in H_2	0.5 wt% CeO_2 rods, cubes and octahedra	1.5–2 nm	1% CO, 1% O_2, and 50% H_2 balanced with N_2	60,000 mL g^{-1} h^{-1}	1	2	60 (r) 100(c) 100(o)	85 60 65	40 45 30	[16]
Impregnation with [Pt(NH3)4](NO3)2	Calcined 500 °C in air Reduced 500 °C in H_2	1 wt%, CeO_2 co-precipitation with excess urea	–	2% CO, 2% O_2, 20% H_2 balanced in He.	GHSV = 17,000 h^{-1}	1	2	120	85	–	[17]
Solution combustion synthesis	Reduction 400 °C in H_2 and PROX cycles	–	2–6 nm	CO:O_2:H_2 2:2:48%	–	1	2	140	95	50	[18]
Impregnation with H_2PtCl_6	Calcined 500 °C in air Reduced 250 °C in H_2	CeO_2 sol–gel	–	20–70% H_2, 2% CO, 2% O_2, 5% CO_2, 5% H_2O and He as a balance	GHSV = 17,000 h^{-1}	1	2	110	80	40	[19, 20]

Table 2 (continued)

Method	Catalyst treatment process before reaction	Pt metal loading (wt%)/CeO2 support	Pt particle size (nm)/dispersion	Feed composition (vol%)	Space velocity or GHSV	O_2/CO feed ratio	λ	T (°C)[a]	CO conversion (%)	CO_2 selectivity (%)	References
Glucose-assisted hydrothermal method	Calcined 350–600 °C in air Reduced 400 °C in H_2	–	6–12 nm	1% CO, 1% O_2, 70% H_2 and He for balance	120,000 mL g^{-1} h^{-1}	1	2	90–100	75–80	40	[21]
Alcohol-reduction Process	No treatment	0.5 wt% Pt, CeO_2 anopowder Sigma-Aldrich	2.2 nm	1% CO, 0.5–1% O_2, 97.5–98 vol% H_2	30,000 mL g_{cat}^{-1} h^{-1} 15,000 mL g_{cat}^{-1} h^{-1}	0.5 1	1 2	50 50	81 98	73 46	This work

[a]Temperature of maximum CO conversion

are fundamental for reactions like CO oxidation and CO-PROX reaction. Besides that, also the presence of noble metals can change the CeO_2 surface properties, weakening Ce–O bond, and making the surface more reducible. The study of Pt nanoparticles dispersed on nanosized CeO_2 active at room temperature for CO oxidation using different techniques revealed that elongated Pt–O distance resulting from the interaction of Pt species with CeO_2 in the form of low-temperature active species–support interaction. Gao et al. [16] also observed for Pt/CeO_2 prepared by impregnation that the Pt precursor interacts in different ways with CeO_2 supports with different morphologies resulting in catalysts with different fractions of metallic Pt and Pt^{2+} species. Moreover, the promoting effect of Pt on the reducibility of CeO_2 supports and the concentration of oxygen vacancies varied with CeO_2 morphology and Pt–CeO_2 interaction. Polster et al. [13] studied CO and H_2 oxidation over a series of Pt/CeO_2 catalysts with different Pt loadings and dispersion, and showed that interfacial Pt–O–Ce sites are responsible for Mars and van Krevlen redox activity. Recently, Gänzler et al. [26] described that the Pt/CeO_2 interface can be tuning by the variation of the Pt nanoparticle sizes, which determines the number of interfacial sites between Pt nanoparticles and CeO_2. It was demonstrated that the formation of small Pt nanoparticles (in the range of 1 and 2 nm) induces variations in CeO_2 reducibility and this is a prerequisite for CeO_2 reduction at low temperatures. Besides that, the importance of an intimate and optimal interaction between Pt and CeO_2 activates the redox chemistry that is important for applications involving high oxygen storage capacity and enhanced low-temperature CO oxidation.

Conclusions

Pt/CeO_2 catalysts with Pt contents of 0.5 and 1wt% and average nanoparticles sizes of 2.2 and 2.4 nm could be prepared by a facile methodology. The obtained catalysts showed to be active, selective, and stable at 50 °C for CO-PROX reaction. This activity at low temperature could be a result of the optimal interaction of the small-sized Pt nanoparticles and CeO_2 nanoparticles used as support leading to a weakening of the CO adsorption on Pt sites and favoring O_2 adsorption/activation on active redox sites at Pt/CeO_2 interfaces.

Acknowledgements FAPESP/Shell Proc. nº 2014/50279-4 (RCGI) and 2017/11937-4 (CINE); FAPESP Proc. nº 2014/09087-4, 2017/15469-5, and 2018/04802-8; and CNPq Proc. nº 304869/2016-3 are grateful for financial support. Centro de Ciência e Tecnologia dos Materiais (CCTM), IPEN-CNEN/SP are acknowledged for the use of TEM facilities.

References

1. Saavedra, J., Whittaker, T., Chen, Z., Pursell, C.J., Rioux, R.M., Chandler, B.D.: Controlling activity and selectivity using water in the Au-catalysed preferential oxidation of CO in H_2. Nat. Chem. **8**, 584–589 (2016)
2. Liu, K., Wang, A., Zhang, T.: Recent advances in preferential oxidation of CO reaction over platinum group metal catalysts. ACS. Catal. **2**, 1165–1178 (2012)
3. Yu, X., Li, H., Tu, S.-T., Yan, J., Wang, Z.: PteCo catalyst-coated channel plate reactor for preferential CO oxidation. Int. J. Hydrog. Energy **36**, 3778–3788 (2011)
4. Ashraf, M.A., Ercolino, G., Specchia, S., Specchia, V.: Final step for CO syngas clean-up: comparison between CO-PROX and CO-SMET processes. Int. J. Hydrog. Energy **39**, 18109–18119 (2014)
5. Ercolino, G., Ashraf, M.A., Specchia, V., Specchia, S.: Performance evaluation and comparison of fuel processors integrated with PEM fuel cell based on steam or autothermal reforming and on CO preferential oxidation or selective methanation. Appl. Energy **143**, 138–153 (2015)
6. Nematollahi, B., Rezaei, M., Lay, E.N.: Preparation of highly active and stable NiO-CeO_2 nanocatalysts for CO selective methanation. Int. J. Hydrog. Energy **40**, 8539–8547 (2015)
7. Gao, Z., Cui, L., Ma, H.: Selective methanation of CO over Ni/Al2O3 catalyst: effects of preparation method and Ru addition. Int. J. Hydrog. Energy **41**, 5484–5493 (2016)
8. Wootsch, A., Descorme, C., Duprez, D.: Preferential oxidation of carbon monoxide in the presence of hydrogen (PROX) over ceria–zirconia and alumina-supported Pt catalysts. J. Catal. **225**, 259–266 (2004)
9. Ayastuy, J.L., Gil-Rodríguez, A., González-Marcos, M.P., Gutiérrez-Ortiz, M.A.: Effect of process variables on Pt/CeO_2 catalyst behaviour for the PROX reaction. Int. J. Hydrog. Energy **31**, 2231–2242 (2006)
10. Pozdnyakova, O., Teschner, D., Wootsch, A., Kröhnert, J., Steinhauer, B., Sauer, H., Toth, L., Jentoft, F.C., Knop-Gericke, A., Paál, Z., Schlögl, R.: Preferential CO oxidation in hydrogen (PROX) on ceria supported catalysts PART I. Oxidation state and surface species on Pt/CeO_2 under reaction conditions. J. Catal. **237**, 1–16 (2006)
11. Teschner, D., Wootsch, A., Pozdnyakova, O., Sauer, H., Knop-Gericke, A., Schlögl, R.: Surface and structural properties of Pt/CeO_2 catalyst under preferential CO oxidation in hydrogen (PROX). React. Kinet. Catal. Lett. **87**, 235–247 (2006)
12. Teschner, D., Wootsch, A., Pozdnyakova-Tellinger, O., Kröhnert, J., Vass, E.M., Hävecker, M., Zafeiratos, S., Schnörch, P., Jentoft, P.C., Knop-Gericke, A., Schlögl, R.: Partial pressure dependent in situ spectroscopic study on the preferential CO oxidation in hydrogen (PROX) over Pt/ceria catalysts. J. Catal. **249**, 318–327 (2007)
13. Polster, C.S., Zhang, R., Cyb, M.T., Miller, J.T., Baertsch, C.D.: Selectivity loss of Pt/CeO_2 PROX catalysts at low CO concentrations: mechanism and active site study. J. Catal. **273**, 50–58 (2010)
14. Kugai, J., Moriya, T., Seino, S., Nakagawa, T., Ohkubo, Y., Nitani, H., Daimon, H., Yamamoto, T.A.: CeO_2-supported PtCu alloy nanoparticles synthesized by radiolytic process for highly selective CO oxidation. Int. J. Hydrog. Energy **37**, 4787–4797 (2012)
15. Liu, Y., Liu, B., Liu, Y., Wang, Q., Hu, W., Jing, P., Liu, L., Yu, S., Zhang, J.: Improvement of catalytic performance of preferential oxidation of CO in H_2-rich gases on three-dimensionally ordered macro- and meso-porous Pt–Au/CeO_2 catalysts. Appl. Catal. B Environ. **142–143**, 615–625 (2013)
16. Gao, Y., Wang, W., Chang, S., Huang, W.: Morphology effect of CeO2 support in the preparation, metal-support interaction, and catalytic performance of Pt/CeO2 catalysts. ChemCatChem **5**, 3610–3620 (2013)
17. Jardim, E.O., Rico-Francés, S., Coloma, F., Anderson, J.A., Ramos-Fernandez, E.V., Silvestre-Albero, J., Sepúlveda-Escribano, A.: Preferential oxidation of CO in excess of H_2 on Pt/CeO_2–Nb_2O_5 catalysts. Appl. Catal. A **492**, 201–211 (2015)
18. Nguyen, T.S., Morfin, F., Aouine, M., Bosselet, F., Rousset, J.L., Piccolo, L.: Trends in the CO oxidation and PROX performances of the platinum-group metals supported on ceria. Catal. Today **253**, 106–114 (2015)
19. Rico-Francés, S., Jardim, E.O., Wezendonk, T.A., Kapteijn, F., Gascon, J., Sepúlveda-Escribano, A., Ramos-Fernandez, E.V.: Highly dispersed Ptδ + on $Ti_xCe_{(1-x)}O_2$ as an active phase in preferential oxidation of CO. Appl. Catal. B Environ. **180**, 169–178 (2016)
20. Rico-Frances, S., Sepulveda-Escribano, A., Ramos-Fernandez, E.V.: $Ti_xCe_{(1-x)}O_2$ as Pt support for the PROX reaction: effect of the solvothermal synthesis. Int. J. Hydrog. Energy **42**, 29262–29273 (2017)
21. Carvalho, D.R., Aragão, I.B., Zanchet, D.: Pt-CeO_2 catalysts synthesized by glucose assisted hydrothermal method: impact of calcination parameters on the structural properties and catalytic performance in PROX-CO. J. Nanosci. Nanotechnol. **18**, 3405–3412 (2018)
22. Oliveira Neto, A., Dias, R.R., Tusi, M.M., Linardi, M., Spinacé, E.V.: Electro-oxidation of methanol and ethanol using PtRu/C, PtSn/C and PtSnRu/C electrocatalysts prepared by alcohol-reduction process. J. Power Sources **166**, 87–91 (2007)
23. Ivanov, I., Petrova, P., Georgiev, V., Batakliev, T., Karakirova, Y.V., Serga, V., Kulikova, L., Eliyas, A., Rakovsky, S.: Comparative study of ceria supported nano-sized platinum catalysts synthesized by extractive-pyrolytic method for low-temperature WGS reaction. Catal. Lett. **143**, 942–949 (2013)
24. Paz, D.S., Damyanova, S., Borges, L.R., Santos, J.B.O., Bueno, J.M.C.: Identifying the adsorbed active intermediates on Pt surface and promotion of activity through the redox CeO_2 in preferential oxidation of CO in H_2. Appl. Catal. A General **548**, 164–178 (2017)
25. Gatla, S., Aubert, D., Agostini, G., Mathon, O., Pascarelli, S., Lunkenbein, T., Willinger, M.G., Kaper, H.: Room-temperature CO oxidation catalyst: low-temperature metal-support interaction between platinum nanoparticles and nanosized ceria. ACS Catal. **6**, 6151–6155 (2016)
26. Gänzler, A.M., Casapu, M., Maurer, F., Störmer, H., Gerthsen, D., Ferré, G., Vernoux, P., Bornmann, B., Frahm, R., Murzin, V., Nachtegaal, M., Votsmeier, M., Grunwaldt, J.-D.: Tuning the Pt/CeO_2 interface by in situ variation of the Pt particle size. ACS Catal. **8**, 4800–4811 (2018)